C. R. Geoscience 349 (2017) 165–174

Contents lists available at ScienceDirect

Comptes Rendus Geoscience

www.sciencedirect.com

Hydrology, environment

Petrology and geochemistry of REE-rich Mafé banded iron formations (Bafia group, Cameroon)

Charles Nkoumbou [a,*], Fuh Calistus Gentry [a,b], Jacqueline Tchakounte Numbem [a], Yolande Vanessa Belle Ekwe Lobé [a], Christin Steve Nwagoum Keyamfé [a]

[a] Department of Earth Sciences, Faculty of Science, The University of Yaoundé-I, P.O. Box 812, Yaoundé, Cameroon
[b] Ministry of Mine, Industry and Technology Development, Yaoundé, Cameroon

ARTICLE INFO

Article history:
Received 14 January 2017
Accepted after revision 31 March 2017
Available online 2 August 2017

Handled by François Chabaux

Keywords:
Bafia
Cameroon
BIF (Banded Iron Formation)
Geochemistry
Petrology

ABSTRACT

Archaean–Paleoproterozoic foliated amphibole-gneisses and migmatites interstratified with amphibolites, pyroxeno-amphibolites and REE-rich banded-iron formations outcrop at Mafé, Ndikinimeki area. The foliation is nearly vertical due to tight folds. Flat-lying quartz-rich mica schists and quartzites, likely of Pan-African age, partly cover the formations. Among the Mafé BIFs, the oxide BIF facies shows white layers of quartz and black layers of magnetite and accessory hematite, whereas the silicate BIF facies is made up of thin discontinuous quartz layers alternating with larger garnet (almandine–spessartine) + chamosite + ilmenite ± Fe-talc layers. REE-rich oxide BIFs compositions are close to the East Pacific Rise (EPR) hydrothermal deposit; silicate BIFs plot midway between EPR and the associated amphibolite, accounting for a contamination by volcanic materials, in addition to the hydrothermal influence during their oceanic deposition. The association of an oceanic setting with alkaline and tholeiitic magmatism is typical of the Algoma-type BIF deposit. The REE-rich BIFs indices recorded at Mafé are interpreted as resulting from an Archaean–Paleoproterozoic mineralization.

1. Introduction

Iron ore formations occur in cratons worldwide and constitute huge deposits. They precipitated in the hydrosphere (Simonson, 2003) during the Archaean time (3850–2500 Ma) and the Early Proterozoic (2500–1600 Ma) era. The maximum deposition took place between 2300 and 1900 Ma (Klein, 2005). Their texture is either granular or banded; the latter is locally known as itabirites, taconites or jaspilites. The term Banded Iron Formation, i.e. BIF, refers to sedimentary iron-rich layers generally alternating with silica-rich layers or their metamorphic equivalent (Trendall, 1983). In addition to their great interest due to their importance as the world's largest source of iron ore (Robb, 2005), BIF study aims at key aspects such as their composition, classification and genesis, their temporal and spatial distributions, the different facies associations and depositional and the reconstitution of the early Earth's evolution (Gonzalez et al., 2009; Klein, 2005).

Many important banded iron formations (BIF) and other iron ore deposits exist in the Achaean Ntem complex (also known as greenstone belt), near the northern edge of the Congo Craton, which crops out in southern Cameroon. For example, the Mbalam iron ore district hosts over 220 Mt of iron ore with Fe more than 60% corresponding to Direct Schipping Ore, and more than 2.4 Bt of ore with 25 to 60% Fe; the Mamelles deposit hosts about 350 Mt of ore with a mean composition of 30% Fe. In addition to this main

* Corresponding author.
E-mail address: nkoumbouc@yahoo.fr (C. Nkoumbou).

http://dx.doi.org/10.1016/j.crte.2017.03.002
1631-0713/

deposits, other BIFs and iron ore deposits and prospects (Fig. 1) are known in the Archaean-Paleoproterozoic Congo craton such as Nkout, Ngoua, Mewongo, Njweng, Nkom-Akak, Bikoula, Sangmelima, Kouambo, Zambi and Eseka to the south (Chombong and Suh, 2013; Chombong et al., 2013; Ganno et al., 2015a; Ilouga et al., 2013; Nforba et al., 2011; Suh et al., 2008, 2009; Tessontsap Teutsong et al., 2017); Kribi and Edéa to the west (Ganno et al., 2015b, 2017); Touboro and Vaïmba in the Adamawa in the Centre Cameroon and Mayo Binka in the Pan-African formations in the North-West region of Cameroon (Suh et al., 2008).

When the banded-iron formations prospects were recently discovered at Mafé, at about 26 km west of Ndikinimeki, we decided to promptly provide preliminary mineralogical and geochemical data. At the onset, the questions arising were:

- what are the relationships between the different geological formations hosting the BIFs prospects;
- what are the characteristics of the BIFs;
- what was the geotectonic context at the deposition;
- to which type, i.e. Algoma- or Superior-type, do the prospects belong?

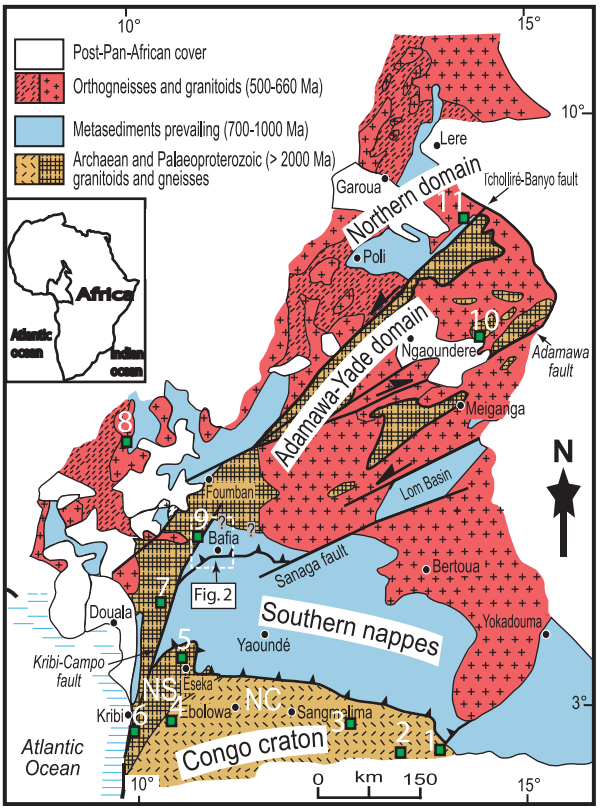

Fig. 1. Geological map of Cameroon (modified from Nkoumbou et al., 2014) showing known and newly discovered iron-ore deposits and prospects. 1: Mbalam; 2: Nkout; 3: Sangmelima; 4: Kouambo; 5: Ngovayang (Eseka); 6: Mamelles (Kribi); 7: Kopongo (Edéa); 8: Kimbi River; 9: Mafé (Ndikinimeki); 10: Touboro; 11: Vaïmba, NC: Ntem complex, NS: Nyong series. The insert shows the location of Cameroon in Africa.

Our paper presents preliminary data on field cartography, petrological and geochemical analyses of the BIFs and their country rocks which, we hope, will highlight the economic potential of Ndikiniméki area, leading thus to further studies in this locality.

2. Geological setting

Mafé is located at about 300 km north of the Archaean Congo craton. It corresponds to the western part of the Bafia area and as such, belongs to the Adamawa–Yade domain (Tchakounté et al. submitted), which has been assigned to the Pan-African Central African Fold Belt (CAFB) in Cameroon (e.g., Bouyo Houketchang et al., 2009; Ngako and Njonfang, 2011; Ngako et al., 2008, 1991; Ngnotué et al., 2000; Tchakounté et al., 2007; Toteu et al., 2001). Moreover, recent studies show that the Adamawa–Yade is an Archaean micro-continent that separated from the Congo craton during the Early Neoproteozoic rifting (Nkoumbou et al., 2014; Tchakounté et al., submitted). According to Tchakounte et al. (submitted), the Bafia area is made up of migmatitic gneiss of Archaean (U-Pb: 2980 ± 36 Ma) and Palaeoproterozoic (2081 ± 26 Ma to 2073 ± 20 Ma) ages (Fig. 2). It consists of medium-grained (0.5–1.5 mm) grey migmatitic gneiss displaying a granoblastic texture. Sample chemistry shows all the features of Archaean Tonalite–Trondjhemite–Granite, i.e. TTG (see Martin et al., 2005 and Moyen and Martin, 2012) as indicated

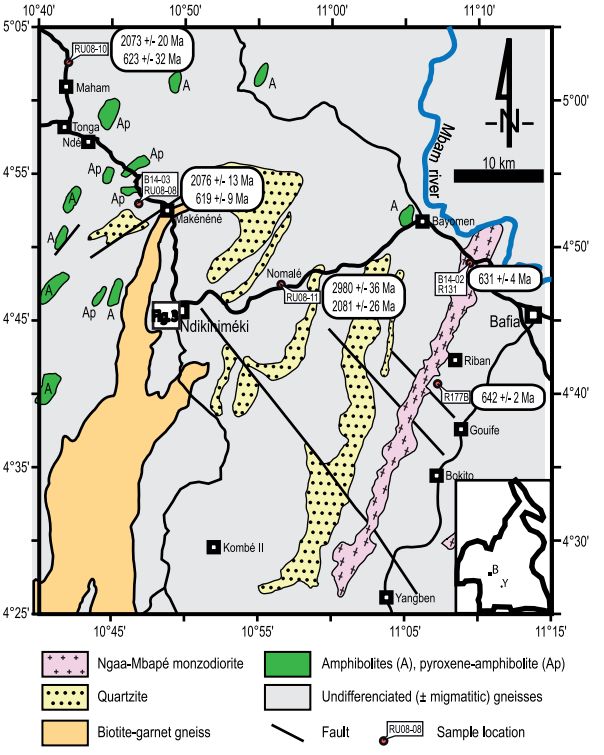

Fig. 2. Map of Bafia area showing the geological setting of Mafé BIF prospects. Right lower insert: location of Bafia area in Cameroon. B: Bafia; Y: Yaoundé. Indicated ages of formations are from Tchakounte et al. (accepted).

by Nd isotopic data, i.e. positive $\varepsilon_{Nd(2.5\ Ga)}$ value (1.7) and an Archaean Nd model age (T_{DM} = 2.5 Ga, Toteu et al., 2001). More than a dozen of km-size amphibolite, pyroxene-amphibolite and pyroxenite massifs are embedded in the migmatitic gneiss. The amphibolite is made up of hornblende, andesine and microcline porphyblasts displaying undulatory extinction and surrounded by a fine-grained groundmass comprised of amphibole, orthoclase, opaque oxides, apatite and zircon. Pyroxene-amphibolite and pyroxenite displaying granular or porphyritic textures are made up of Mg-hypersthene, edenitic and pargasitic hornblende, biotite, almandine-pyrope rich garnet and oligoclase (Tchato, 2013). Both amphibolite and pyroxenite massifs are Palaeoproterozoic in age (U–Pb on zircon: 2067–2041 ± 20 Ma, Tchouankoué, personal communication, 2016) as the surrounding migmatitic gneiss (see Fig. 2). In addition, Tchakounté (1999) found that the Bafia formations are Archaean in age as syndepositional amphibolites display Sm–Nd model ages ranging from 3.3 to 3.0 Ga, and from 3.3 to 2.3 Ga for metagrauwackes and metapelitic rocks, respectively. The Sm–Nd data were challenged until recently when U–Pb dating of gneiss zircons (Fig. 2) yielded Archaean and Paleoproterozoic ages. Interstratified gneisses and embedded mafic-ultramafic rocks are intruded by Neoproterozoic granitoids (U–Pb: 642 ± 2 Ma at Bep, 619 ± 9 Ma at Maham) and monzodiorite–syenite (U–Pb: 631 ± 4 Ma at Gaah Bapé, Toteu et al., 2006; Tchakounté et al. submitted). At the western part of Bafia, banded iron ore formations are interbedded with migmatitic gneiss and amphibolite, which are characterized by NE-trending steep folded foliation. All the formations south of Ndikinimeki, are overlain by discordant Pan-African biotite–garnet micaschist and quartzite displaying horizontal or gently folded (deep < 15°) schistosity.

3. Geology of the Mafé banded iron formations

Mafé area is made up of migmatitic gneisses embedding banded iron formations and amphibolites (Fig. 3). The migmatitic gneisses foliation is outlined by alternating dark and white layers, made up of biotite ± amphibole, and of orthoclase and quartz ribbons, respectively. Folding generated tight anticlinal and synclinal structures at the regional scale. Foliation trends NE–SW (N25-48°E) and dips vertically, or either 45–65 NW or 56–70 SE. In Mafé, banded iron formations and amphibolites outcrop as 100 m lenses likely parallel to the foliation. Banding in the iron formations is metric or centimetric in thickness at the outcrop scale. West of Mafé, outcrops of BIF display centimetre-thick foliation made up of alternating ochre layers with discontinuous white quartz layers and after the Molo River, a few BIF black metric boulders show millimetre-thick quartz laminae (Fig. 4).

4. Sampling and analytical methods

The study area is covered with a thick alteration mush in a rain forest, an impenetrable jungle. Observations and sampling were made possible thanks to road track levelling and along riverbeds. This study is based on a selection of seven banded iron formations, three

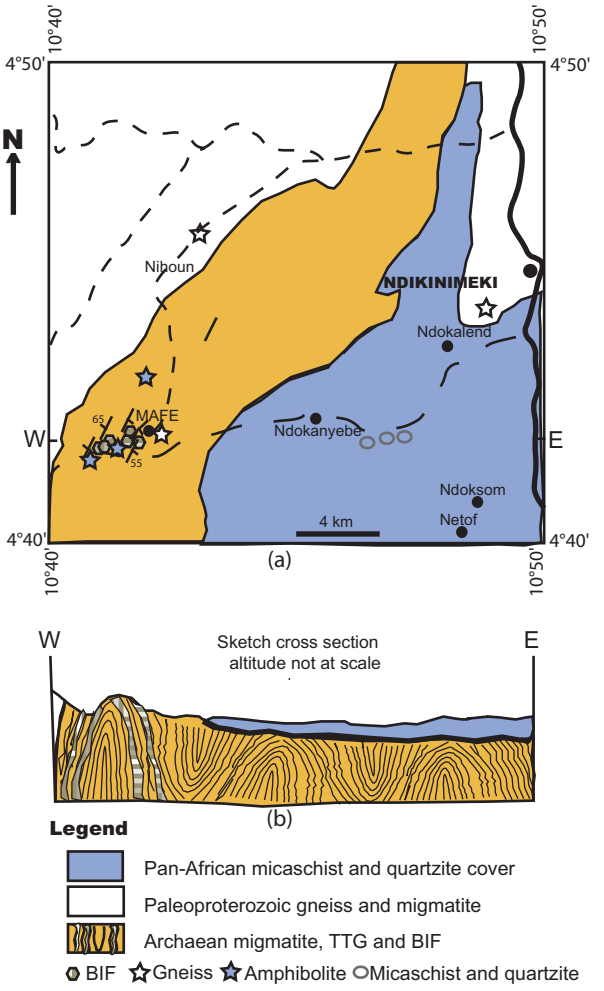

Fig. 3. Geological map (a) and cross-section (b) of Mafé area.

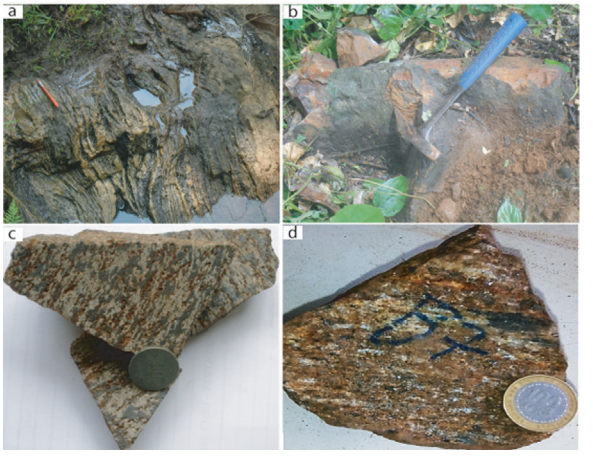

Fig. 4. Photographs of outcrops and samples. a: migmatitic gneiss showing steep slope foliation; b: boulder of oxide BIF in the forest; c & d: samples of oxide BIF.

amphibolites, one gneiss, and one micaschist sample. Thin sections of all samples were realized at the "Centre de recherches pétrographiques et géochimiques" (CRPG, Nancy, France) and at the Institute of Geological Research and Mining, Yaoundé, Cameroon. X-ray diffraction of BIF sample was performed at the Local Material Promotion Authority or 'Mission de promotion des matériaux locaux', i.e. MIPROMALO (Yaoundé, Cameroon) by reflection on random powders, with a Bruker D8 Advance device, using the Co Kα radiation (λ = 1.789 Å), under 35 kV and 45 mA operating conditions. The data were recorded between 5° and 60° (2θ) for whole-rock samples, 0.036° step scan, 3.0 s step time.

Mineral compositions were analysed with an automated CAMECA SX100 electron microprobe (Université de Lorraine, Nancy, France). Operating conditions for silicates and oxides were as follows: 15 kV acceleration voltage/20 nA probe current, with 10 s counting time for Ca, Ti, Mn, and 5 s for Na and K. Natural and synthetic oxides and metallic elements were used as standards and the raw data were corrected using CAMECA X-PHI program (Nkoumbou et al., 2009). Major and trace element compositions were analysed by ICP-AES and ICP-MS at ALS Minerals Global Group, Vancouver (Canada), respectively. Representative samples were pulverized and homogenized, of which 50–60 g were used for the analyses. Loss on ignition (LOI) was determined by weight difference after ignition at 1000 °C; 0.2 g of rock powder was fused with 1.5 g $LiBO_2$ and then dissolved in 100 mL 5% HNO_3. Data quality was checked by running various standards between samples. Analytical uncertainties vary from 0.1% to 0.04% for major elements; and 0.1 to 0.5% for trace elements. The detection limit for REE and Y was 0.01 ppm.

5. Petrography

5.1. The Pan-African cover formations

Quartz-rich micaschist south of Ndikinimeki displays a lepidogranoblastic texture made up of abundant biotite crystals (30–40 vol.%) associated with muscovite, surrounding phenoblasts of plagioclase (< 5 vol.%), orthoclase (10 vol. %) and microcline (5 vol.%). Quartz (20–30 vol. %) occurs as phenoblasts displaying undulatory extinction or as microblasts associated with muscovite. Inclusions of accessory zircon crystals and opaque minerals are observed in the phenoblasts.

5.2. BIF's country rocks: migmatitic gneiss and amphibolite

Migmatitic gneisses and amphibolites are associated with the BIFs.

Dark green amphibolite with heterogranular nematoblastic texture is made up of abundant amphibole (35–45 vol.%) associated with plagioclase (10 vol.%), K-feldspar (15 vol.%) and quartz crystals. Amphibole retrogression yields secondary biotite, muscovite and quartz. A titanite coronitic microtexture developed at the expense of the opaque minerals. The rock is occasionally crosscut by centimetre-thick quartz-feldspar veins. Migmatitic biotite-gneisses and amphibole-biotite gneisses display a clear foliation marked by thin dark layers made up of biotite or amphibole, biotite and opaque minerals, alternating with thicker white layers of K-feldspar, plagioclase and quartz. In biotite-gneisses, plagioclase is pseudomorphosed by muscovite and quartz, whereas orthoclase and biotite retrogression yields microcline and chlorite, respectively. Retrometamorphism is acute in amphibole–biotite gneisses, and amphibole is replaced by secondary biotite, muscovite, chlorite, quartz and opaque minerals. The secondary minerals form patches, which emphasize the grano-nemato-lepidoblastic texture of the rock.

5.3. BIFs

Two main types of BIF iron ore samples occur in the Mafé area. First, the oxide BIF facies is characterized by discontinuous alternating white quartz-rich and dark iron oxide layers (Fig. 5a). The rock strongly attracts the magnetic pen. Under the transmitted light polarizing microscope, the texture appears granoblastic heterogranular with the mineralogical layering defined by 50–55 vol.% of magnetite occasionally rimmed by hematite, and 50–45 vol.% of quartz. Opaque minerals occur as continuous and discontinuous trails accompanied by quartz phenoblasts displaying undulatory extinction. Quartz microblasts are usually associated with hematite crystals (Fig. 5b). Reflected light microscope was not available during this study.

The second BIF type, a silicate facies, does not attract the magnetic pen. White quartz and dark garnet + phyllite layers generate the rock heterogranular grano-lepidoblastic texture (Fig. 5c). Quartz (almost 30–40 vol.%) occurs as sub-angular phenoblasts forming thin layers compared to dark garnet ones (Fig. 5c). Garnet crystals (50–60 vol.%) occur as sub-rounded jointed phenoblasts in dark layers or

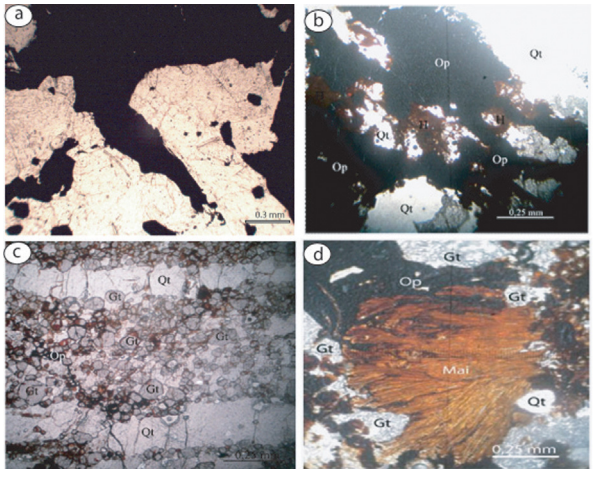

Fig. 5. Photomicrographs of the BIFs. a: dark and white layers of hematite and quartz, respectively (plane polarized light); b: relationship between hematite–magnetite-quartz (plane polarized light); c: granoblastic texture of silicate BIF (plane polarized light); d: Fe-chlorite in silicate BIF (plane polarized light).

as round microblasts with black rim. The dark layer also includes magnetite, hematite and quartz microblasts. Opaque minerals sometimes, fill interstices, which cross-cut the rock foliation. Phyllite minerals, i.e. Fe-chlorite and, probably minnesotaïte, are less abundant (5 vol.%) and appear as flakes < 0.5 mm in size always associated with oxides (Fig. 5d).

X-ray diffraction confirms that oxide BIFs are mainly made up of magnetite, hematite, and quartz with small diffractions ascribed to traces of Fe-talc, Fe-chlorite and garnet (Fig. 6a), whereas silicate BIFs are comprised of garnet, quartz, magnetite, ilmenite, hematite, Fe-chlorite, Fe-talc, annite, and apatite (Fig. 6b).

6. Mineralogy

Microprobe analyses were performed on amphibole-gneisses (BIF country rock) and on the silicate facies of the BIFs. Data were obtained on plagioclase, amphibole, orthoclase, garnet, ilmenite and Fe-chlorite (Table SM1).

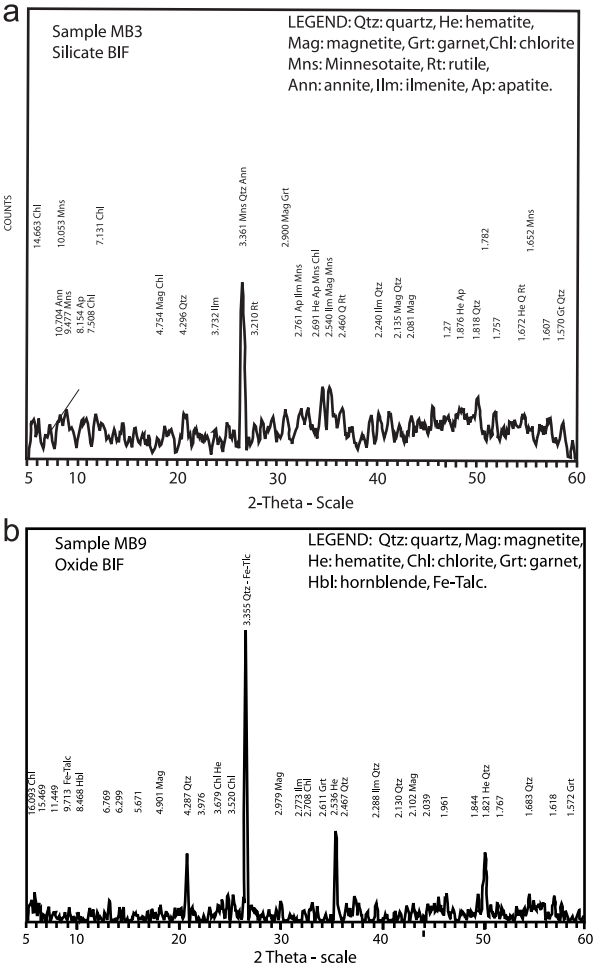

Fig. 6. XRD patterns of Mafé BIFs. a: silicate BIF facies; b: oxide BIF facies.

6.1. Country rocks

In amphibole gneiss, plagioclase composition ranges from andesine to oligoclase ($Ab_{73\text{-}64}An_{34\text{-}26}Or_{01}$), and displays a reverse zoning. K-feldspar is orthoclase ($An_0Ab_{5.51}Or_{94.49}$). Amphibole crystals are potassian magnesio-hastingsite and potassian hastingsite, from the core to the rim, respectively (Leake et al., 1997).

6.2. Silicate BIFs facies

Garnet composition in the silicate BIFs facies is at middle point on the almandine–spessartine joint with accessory molecules of pyrope, grossular, and andradite ($Alm_{42.6\text{-}40.3}Sp_{40.3\text{-}38.9}Py_{13\text{-}12.4}Gro_{6.5\text{-}6.1}And_{6.7\text{-}1.0}Uv_0$). Mg + Fe-rich chlorite is made up of 37% clinochlore and 63% chamosite. Ilmenite is manganoan. A peculiar feature of this mineral assemblage is the great partition of manganese into garnet and ilmenite lattices, i.e. 17.5 and 12.9 wt. % MnO, respectively. The chlorite manganese content is low, i.e. MnO: 0.3 wt. %. The assemblage garnet-chlorite–ilmenite–quartz in the BIFs associated with the amphibole-biotite-andesine paragenesis in the country rock, indicates a medium to high grade metamorphism (Klein, 2005). More mineralogical data are needed for a thorough quantification of the metamorphic processes that prevailed in the Mafé area.

7. Geochemistry

Twelve samples (seven BIFs, three amphibolites, one migmatitic gneiss and one micaschist) were analysed for major and trace elements including rare-earth elements. Results and selected analyses of other BIF prospects and deposits in Cameroon are presented in Table SM2.

7.1. Country rocks

The cover micaschist occurring south of Ndikiniméki shows high SiO_2/Al_2O_3 (4.45) and K_2O/Na_2O (1.93) values in accordance with abundant quartz and biotite. The high Fe_2O_3 (6.45 wt%) content is related to abundant opaque minerals and biotite. In the geochemical classification diagrams by de la Roche (1965) and Herron (1988) (not shown), it plots in the shale field and at the border between shales and greywackes. The low value of chemical index of alteration (CIA = 0.54) and Ba, Cr, Li, Nb, Ni, Rb, Sc, Sr, Ta, Th, U, V, Y, Zn, Zr, and REE high contents indicate that micaschist is derived from immature sediments (Nesbitt and Young, 1982). Mafé migmatitic gneiss is silica-rich (SiO_2: 69.5 wt%), sodic (5.01 wt%), high-aluminium (Al_2O_3: 15.9 wt%), leucocratic (low sum of $Fe_2O_3 + MgO + TiO_2 + MnO \approx 4.32 < 5$ wt%) with low K_2O/Na_2O ratio (≈ 0.28), moderate molecular mg# (62.7), high $(La/Yb)_{CN}$ (179) and Sr/Y (268) values. It shows the characteristics of Archaean TTG (Moyen, 2011) as other grey migmatitic gneisses of the Bafia area. The REE pattern (Fig. 7) shows a steep slope with a prominent Eu positive anomaly [$(Eu/Eu^*)_{CN}$: 2.95]. Among trace elements, Ba and Sr contents are high, i.e. 1535 and 482 ppm, respectively, typical of TTG gneisses, followed by Cr, Zr and

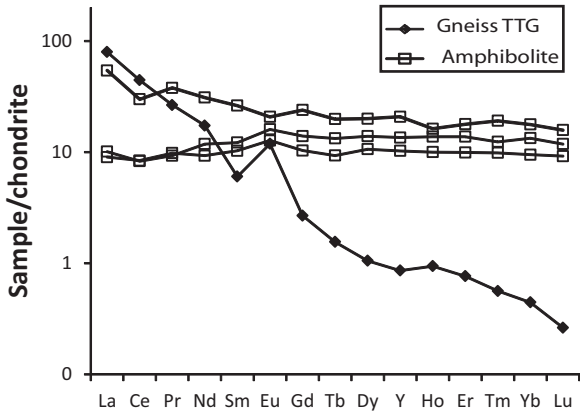

Fig. 7. REE + Y patterns of gneiss and amphibolites.

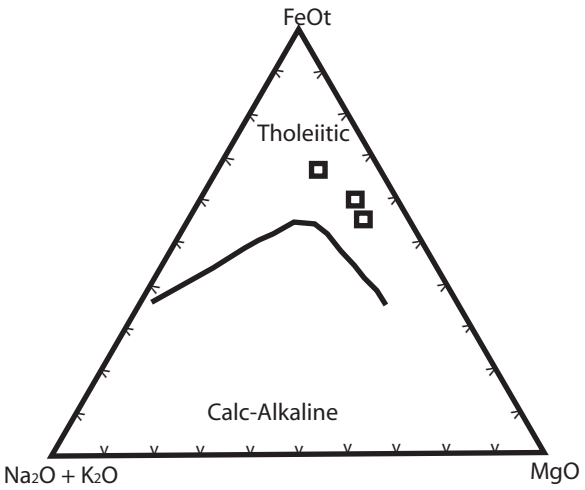

Fig. 8. AFM diagram. Amphibolites plot in the field of tholeiitic rocks.

Zn (Table SM2). Amphibolites probably derived from gabbro and plot in the domain of subalkaline rocks in a TAS diagram (not shown), and in the tholeiite field on the AFM diagram (Fig. 8). REE patterns display a plateau at 10 times chondrite typical of N-MORB (Wilson, 1989) except for a sample enriched in LREE (Fig. 7). Amphibolites are also characterized by weak Eu positive anomalies, i.e. $(Eu/Eu^*)_{CN}$: 1.23, and Ce negative, i.e. $(Ce/Ce^*)_{CN}$: 0.86, anomalies whereas LREE-enriched sample displays Eu negative, i.e. $(Eu/Eu^*)_{CN}$: 0.83, anomaly.

7.2. BIFs

7.2.1. Major oxides

Fe_2O_3 (60.2–32.0 wt.%) and SiO_2 (48.9–31.4 wt.%) are the main oxides. Silicate BIF facies differs from oxide BIF facies by significant amounts of contaminants such as Al_2O_3 (15.5–7.0 vs. 0.68–1.95 wt.%), MgO (5.68–2.31 vs. 0.44–0.05 wt.% except for the oxide BIF facies sample D6 with 5.68 wt% MgO, CaO (1.47–0.66 vs. 0.09–0.04 wt.%), TiO_2 (0.57 vs. 0.26–0.07 wt.%), MnO (0.16 vs. 0.08–0.03 wt%), P_2O_5 (0.24–0.16 vs. 0.19–0.08 wt.%) and LOI (3.6 vs.−0.41 to −0.71 wt.%). The chemical composition of the silicate BIF facies containing large amounts of Al, Ti, Mg, Mn and P can be correlated with the presence of modal garnet (Al, Mg, Mn), chlorite (Al, Mg), ferroan-talc (Mg) and probably, trace of apatite (P). Pecoits et al. (2009) also noticed this feature in the Dales Gorge BIFs in Australia. The oxide BIF facies high iron contents compared with those of silicate BIF facies (60.2–52.1 vs 42.1 wt.%) is related to the alternation of thick opaque magnetite-rich bands with thin quartz-rich ribbons. The compositions of Mafé silicate BIFs are similar to those Gonzalez et al. (2009) described at San Luis (Argentina). Among other studied iron ore prospects and deposits in Cameroon, the Mafé BIFs are similar to the Bikoula BIFs (east of Sangmelima, South Cameroon), which are made up of silicate and oxide facies (Tessontsap Teutsong et al., 2017). On the other hand, the Mafé oxide BIF's show similar compositions with itabirites from well-known iron ore deposits in Cameroon such as those of Mbalam and Elom in the Ntem craton complex (Ganno et al., 2015a; Nforba et al., 2011). In contrast, the silicate BIF facies is distinct with its high contaminant contents. The negative LOI value in oxides BIF facies is due to the abundance of reduce iron (Fe^{2+}) that has likely been oxidized at high temperature, i.e. 1000 °C, during the analytical process. A similar negative LOI value has been reported in banded iron formations from Elom (Ganno et al., 2015b) and Nkout areas (Nsoh et al., 2014) in the Ntem complex, Cameroon.

7.3. Trace elements

BIF silicate facies samples are rich in Ba and Sr, base metals, i.e. As, Co, Cu, Ni, Pb, Sc, Zn and other elements such as V, Y, Zr (Table SM2) reflecting the mineralogy. Base metals and V, Y and Zr show high affinity with magnetite, whereas Ba, Sr, Sc, Nb and Ta may be concentrated in Fe-chlorite (Fedele et al., 2015; Lemarchand et al., 1987). Ferroan-talc is the possible host of Ni, Zn and Co while garnet may host Y, V, Zn, Ba, Sc, Cu, Ni and Co. Ba is concentrated in hematite, magnetite and Fe–Mn oxyhydroxides. Cr and Sr are fitted in the hematite lattice (Pecoits et al., 2009). Data from the oxide BIF facies are very heterogeneous. Some samples (MB9, B7 and D6) are richer in alkaline earths than the BIF silicate facies (Ba: 117–70.8 vs. 50.8–7.3 ppm; Sr: 30.5–12.7 vs. 5.4 ppm, respectively); base metal contents are similar in both silicate and oxide BIF facies, except for high Cu and Sc and low Pb (respectively, 44 vs. 15, 21 vs. 3, and 4 vs. 9 ppm) in the silicate BIFs.

The REE + Y contents in BIFs were normalized to chondrite (subscript: CN) and to Post-Archaean Australian Shale, i.e. PAAS (shale normalized has as subscript: SN). Chondrite and PAAS values are from McDonough and Sun (1995) and from Mclennan (1989), respectively. Y has been inserted between Dy and Ho (Figs. 9a & b), taking into account its ionic radius and its behavior similar to REE (Bau and Dulski, 1999; Gonzalez et al., 2009).

On the chondrite-normalized diagram (Fig. 9a), silicate BIFs present low REE-enrichment and their patterns decrease in a gentle slope from 90–40 (La) to 7–12 (Lu) times chondrite. They display weak to no Ce and Eu

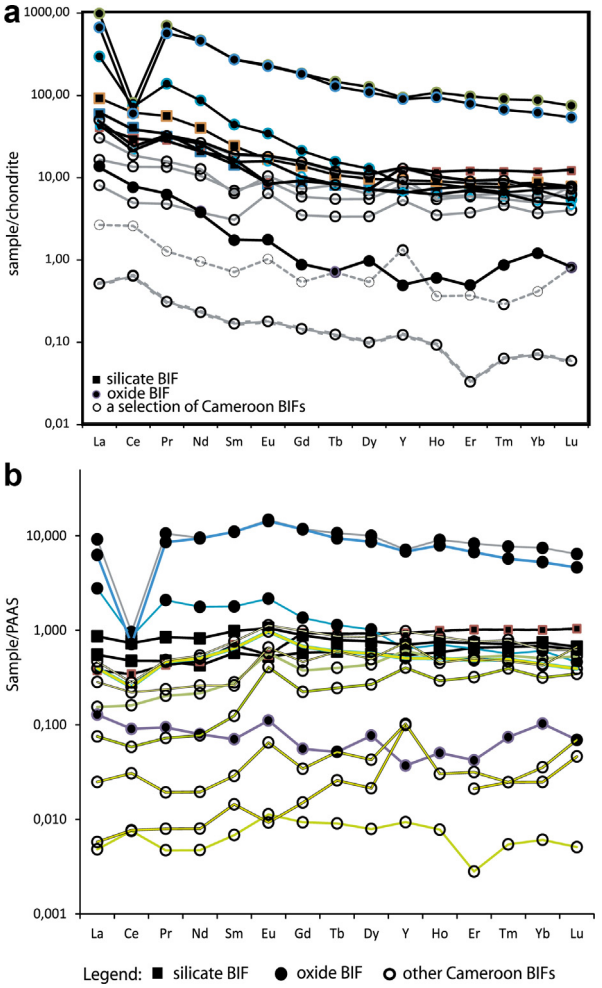

Fig. 9. BIFs REE + Y patterns after normalization to chondrite (a) and to PAAS (b).

negative anomalies, i.e. $(Ce/Ce^*)_{CN}$: 0.86–0.93, and $(Eu/Eu^*)_{CN}$: 0.54–0.91, respectively. The REE and Y contents of silicate BIFs are similar to those of Kouambo, Metzewin and Mbalam BIFs. Unlike silicate BIFs facies, oxide BIFs facies show a large REE enrichment except sample MB5 which presents low REE contents, a weak Ce negative anomaly, i.e. $(Ce/Ce^*)_{CN}$: 0.83, and a moderate Eu positive anomaly, i.e. $(Eu/Eu^*)_{CN}$: 1.43, similar to other Cameroon BIFs. LREE decrease from La to Sm with $La_{CN}/Sm_{CN} = 4.1$ and the pattern forms a plateau at 12 times chondrite from Gd to Lu with $Gd_{CN}/Lu_{CN} = 1.2$. It is worth noting that two samples are strongly REE-enriched so much so that their patterns decrease from 1000 (La) to 73 (Lu) times chondrite. The patterns are marked by deep Ce negative anomalies, i.e. $(Ce/Ce^*)_{CN}$: 0.1. Sample MB9 pattern decreases from $La_{CN} = 447.3$ to $Lu_{CN} = 8.13$; the steep La to Ho slope, with $La_{CN}/Ho_{CN} = 35$, is followed by a gentle curve down to Lu with $Ho_{CN}/Lu_{CN} = 1.6$. It displays an important Ce negative anomaly, i.e. $Ce/Ce^* = 0.38$.

The PAAS-normalized patterns of the studied BIFs are parallel to chondrite-normalized trend at 7–10 orders at lower magnitudes (Fig. 9b). They exhibit the same characteristics as those observed on CN patterns, but the Ce and Eu anomalies in PAAS-normalized ones are weak. The fact that the REE contents of silicate BIFs are similar to PAAS REE contents is a peculiar feature, thus their patterns form a plateau with very weak or no Ce and Eu anomalies, i.e. 0.83–0.91 and 0.7–1.1, respectively. These patterns overlap or are close to the Kouambo, Metzewin and Mbalam BIFs (Fig. 9b). The patterns of high REE-enriched oxide BIFs form a plateau at 10 times PAAS with a 0.08–0.09 Ce negative anomaly, and exceptionally 0.36 for sample MB9. Conversely, the pattern of MB5 oxide BIF sample displays a plateau at 0.1 time PAAS with a 0.83 limited Ce negative anomaly.

8. Discussion

According to Suh et al. (2008), economic geology investigations of iron ore deposits often seek to answer a number of questions such as:

- the depositional age given that most BIFs were formed when the earth's oxygen was still at low level (Chombong and Suh, 2013; Kaufman et al., 2007);
- the age relationships of magnetite and hematite (Suh et al., 2008 and references therein);
- the age and evolution of the metamorphism (Gonzalez et al., 2009);
- the nature of ore-forming process, i.e. whether it was hypogene and/or hydrothermal and/or supergene);
- the origin of the chemical components and type of depositional environments;
- the relation with other iron ore deposits at a regional scale.

Our discussion of Mafé BIFs preliminary data focuses on:

- the paragenetic sequences;
- the origin of the chemical components and the depositional environments;
- tectonic setting-classification, implications for regional geology.

8.1. Paragenetic sequence

Silicate BIF facies is made up of quartz ribbons alternating with bands of garnet, Fe-chlorite, Fe-talc and a few iron oxides, whereas in oxide BIF facies the dark bands are made up only of magnetite and hematite. Such texture has been assigned to variable pCO_2 (Konhauser et al., 2007) or to the turbiditic flows during deposition (Pickard et al., 2004). Pecoits et al. (2009) proposed that Fe-oxide, chert-siderite-talc and pure chert could represent a diagenetic feature whereby the precipitation/sedimentation of a rather homogenous mass of silica gel was followed by ion diffusion with the consequent segregation of laminae. Unfortunately, this interpretation does not genuinely explain the occurrence of well-bedded BIF in

Mafé. Hence, the association of silicate and oxide BIF facies can be interpreted in terms of precipitation rate variation during the deposition period. Some layers are characterized by clear-cut alternating silica and iron bands, a well-bedded BIF texture known worldwide (Ganno et al., 2015a; Ilouga et al., 2013; Pecoits et al., 2009). In silicate BIF facies, Fe precipitated alone to form iron-bands, and precipitated with silica to form the silica-iron bands where Fe was so scattered that it did not aggregate to form oxides and oxy-hydroxides during the diagenesis and/or metamorphism. Instead, Fe entered the lattices of silicate minerals such as garnet, Fe-chlorite and Fe-talc.

8.2. Source of chemical components and deposition environment

Wonder's et al. (1988) Al_2O_3-SiO_2 diagram discriminates among hydrothermal, hydrogenous and deep-sea sediment environments (Fig. 10a). Silicate facies BIF compositions plot in the hydrogenous field on the diagram, pointing to seawater as the main source of chemical elements precipitating, through chemical reaction between seawater dissolved oxygen and Si + Fe, accordingly with Gonzalez et al. (2009). Oxide facies BIF composition plot in the hydrothermal field, implying that hydrothermal fluids provided Si + Fe. As a whole, the BIFs form a trend suggesting that silicate BIFs could result from the mixing of materials derived from amphibolite protolites and oxide BIFs. REE characteristics of oxide BIF's such as limited or no Eu anomaly and Y positive anomaly, and REE contents similar to PAAS suggest that hydrothermal fluids were low-temperature type (Bau and Dulski, 1999). On a Fe/Ti–Al/Al + Fe + Mn diagram (Bostrom, 1973), Mafé oxide BIF facies is close to uncontaminated modern metalliferous sediments (Al/Al + Fe + Mn < 0.012) despite the low Fe/Ti ratio (< 1000). The silicate BIF facies shows high Al content (Al/Al + Fe + Mn: 0.14) assigned to hydrothermal and volcaniclastic inputs into hydrogenous sediments (Fig. 10b). The trend from oxide to silicate BIFs suggests a possible mixing of metalliferous oceanic sediments with the materials derived from amphibolite protolites. In addition, the heterogeneous enrichment in transition metals such as Cr, Ni, V, Sc (up to 400, 335, 186 and 21 ppm, respectively) and base metals such as Zn and As (up to 169 and 7 ppm, respectively) uphold the hypothesis of contamination by mafic volcanogenic material.

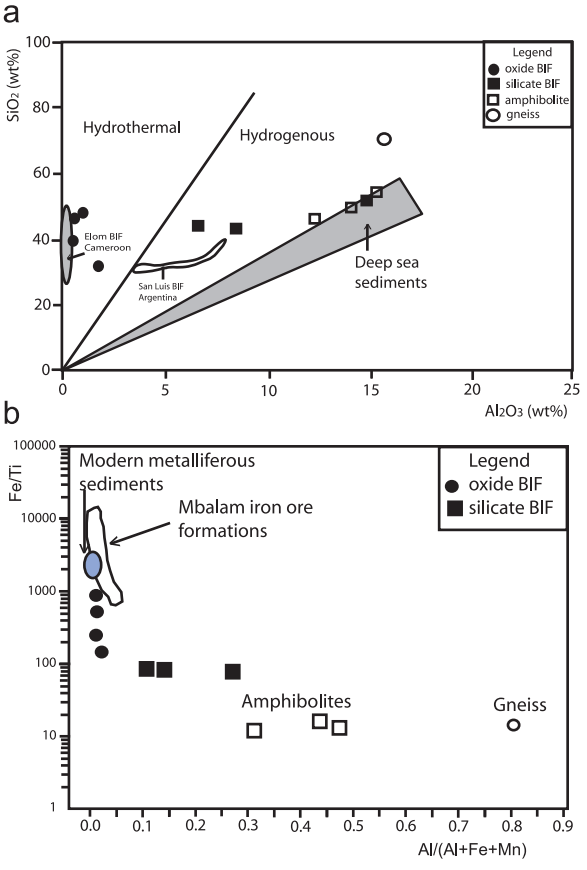

Fig. 10. a: SiO_2 versus Al_2O_3 diagram showing the hydrothermal input in oxide BIFs and hydrogenous input in silicate BIF. For comparison, the ranges of composition of Elom (Ganno et al., 2015a) and San Luis (Gonzalez et al., 2009) BIFs are shown; b: Fe/Ti versus Al/(Al + Fe + Mn) diagram showing a trend from oxide BIF to silicate BIFs. The range of Mbalam iron ore compositions (Nforba et al., 2011) is presented.

The Mafé BIFs REE contents are higher (up to 1090 ppm) than those of other Cameroon BIFs where the values range from 1 to 80 ppm (Elom, Ganno et al., 2015b; Mbalam, Ilouga et al., 2013; Nforba et al., 2011; Nkout, Nsoh et al., 2014). In addition, all samples plot in the field (figure not shown) of negative Ce anomaly (Bau and Dulski, 1996), suggesting an input of oceanic hydrothermal solutions from a deep-sea spreading centre (Ilouga et al., 2013). BIF silicate facies and deep negative anomalies in BIFs oxide facies show no Y/Y* anomalies. On the contrary, silicate BIFs facies have significant Th (0.42–0.82 ppm), Zr (8–18 ppm), Cu (15–44 ppm), Pb (4–9 ppm) and Zn (27–62 ppm) contents, which are likely due to crustal contamination (Gonzalez et al., 2009; Ilouga et al., 2013; Pecoits et al., 2009) or a volcanic input. However, oxide BIFs have low major element contaminants such as Al, Ca, Mg, Na and K. This observation excludes the hypothesis of a volcanoclastic or a detrital material input, although the REE contents are conspicuously high. In addition, REE and other trace elements such as Ba, Co, Cr, Cu, Nb, Ni and Zr are not hosted by silicate minerals, e.g., Fe-talc, chlorite or garnet. Zircon is usually the most frequent host of HREE and Zr (Dymek and Klein, 1988). The Mafé BIFs have the highest Zr content values yet encountered in Cameroon BIFs, i.e. 75–42 ppm. Even though Zr contents of Mayo Binka BIFs are up to 42 ppm, they show $\sum$REE as low as 1.6–5.1 ppm (Suh et al., 2008). Monazite is well known for hosting LREE and Ba. Monazite analyses from Mbalam BIF deposit showed high LREE contents but whole-rock analyses display $\sum$REE values as low as 50 ppm (Ilouga et al., 2013) compared to 1090–914 ppm of the Mafé samples. We conclude that the occurrence of zircon and monazite in Mafé BIFs cannot explain the high REE values and clearly indicates that the origin of the Mafé BIF REE is yet to be determined. Further survey and mineralogical analyses are required.

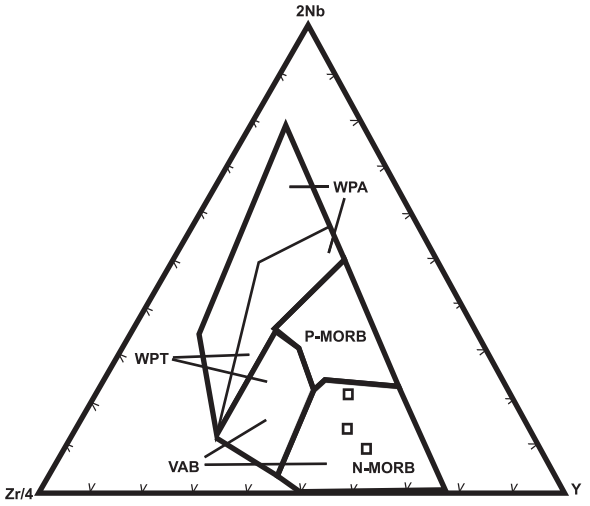

Fig. 11. Zr–Nb–Y (Meschede, 1986) geotectonic discrimination diagram for Mafé amphibolites; N-MORB: normal mid-ocean basalt; P-MORB: plume MORB; VAB: volcanic arc basalt; WPT: within plate tholeiitic basalt; WPA: within plate alkali basalt.

8.3. Tectonic setting and implications for regional geology

A previous study north of Mafé (Tchato, 2013) indicated that amphibolites with Nb/Y = 0.09 were derived from an alkaline protolith, whereas pyroxeno-amphibolites display tholeiitic compositions as pointed out by $K_2O < 0.5$ wt. % and 20 vol. % of $En_{90-65}Fs_{10-35}$ hypersthene. Mafé amphibolites are tholeiitic rocks displaying the characteristics of N-MORB basalts (Fig. 11). The canonical ratios such as La/Nb, i.e. 1.0–2.1 (Condie, 1997) and (Nb/Y: 0.08–0.22 and Zr/Y: 2.3–2.9) values are typical of oceanic tholeiite. The patent heterogeneity of the BIF's compositions, e.g., low Co, Ni, Nb, Ba contents in some samples vs. high contents of Co, Ni, V, Cr, Cu, Hf, REE contents and high Ti/V (18–37) in others, is interpreted in terms of input of mafic alkaline volcanic materials (Nkoumbou et al., 1995; Tchato et al., 2017). Such an association of alkaline and tholeiitic magmatism in oceanic environment probably corresponds to an island arc setting. The combined oceanic precipitation of Fe and Si and the volcanic activity is typical of Algoma-type BIFs deposit (Gross and McLeod, 1980), which is comforted by high Ni, Cr, V, REE and Y contents.

9. Conclusion

Mafé BIF prospects are embedded in amphibole-biotite gneisses and amphibolites of Archaean–Paleoproterozoic age. These formations underwent high-amphibolite to granulitic metamorphism. The BIFs are made up of highly REE-rich oxides and silicates facies, which precipitated in an oceanic environment. They display heterogeneous compositions probably due to interactions among oceanic metalliferous sediments, hydrothermal fluids, and volcaniclastic materials, even though the source of REE is still debatable. The association of an oceanic depositional environment with a significant input of REE, Y and other trace elements from volcanic activity is characteristic of the Algoma-type BIF deposit. At the regional scale, the Mafé BIFs occur along with other BIF deposits and prospects, which extend westwards from Mbalam to Kribi in the Ntem complex, and up to Touboro and Vaïmba, in the Adamawa–Yade cratonic block.

Acknowledgements

The authors are grateful to Pierre Barbey (CRPG-Nancy, France) for microprobe analyses at the 'Université de Lorraine' (Nancy, France). Thanks to Jean-Pierre Tchouankoué (University of Yaoundé-I, Cameroon) who was kind enough to share his unpublished U–Pb isotope data of zircons from the pyroxeno-amphibolite analysed at the University of Sao Paulo (Brazil). We acknowledge the thorough reviews by Dominique Gasquet (Université de Savoie Mont-Blanc, France), José Honnorez (Université de Strasbourg, France) and Rigobert Tchameni (Université de Ngaoundéré, Cameroun) that helped us improve the manuscript. Special thanks go to François Chabaux for the valuable editorial advice.

Appendix A. Supplementary data

Supplementary data associated with this article can be found, in the online version, at http://dx.doi.org/10.1016/j.crte.2017.03.002.

References

Bau, M., Dulski, P., 1996. Distribution of yttrium and rare-earth elements in the Penge and Kuruman iron formations, Transvaal Supergroup, South Africa. Precamb. Res. 79, 37–55.

Bau, M., Dulski, P., 1999. Comparing yttrium and rare earths in hydrothermal fluids from the Mid-Atlantic Ridge: implications for Y and REE behaviour during nearvent mixing and for the Y/Ho ratio of Proterozoic seawater. Chem. Geol. 155, 77–90.

Bostrom, K., 1973. The origin and fate of ferromanganoan active ridge sediments. Stockh. Contrib. Geol. 27, 149–243.

Bouyo Houketchang, M., Toteu, S.F., Deloule, E., Penaye, J., Van Schmus, W.R., 2009. U-Pb and Sm-Nd dating of high-pressure granulites from Tcholliré and Banyo regions: evidence for a Pan-African granulite facies metamorphism in North-Central Cameroon. J. Afric. Earth Sci. 54, 144–154.

Chombong, N.N., Suh, C.E., 2013. 2883 Ma commencement of BIF deposition at the northern edge of the Congo craton, southern Cameroon: new zircon SHRIMP data constraint from metavolcanics. Episodes 36, 47–57.

Chombong, N.N., Suh, C.E., Ilouga, C.D.I., 2013. New detrital zircon U-Pb from BIF-related metasediments in the Ntem complex (Congo craton) of southern Cameroon. Nat. Sci. 5 (7), 835–847.

Condie, K.C., 1997. Source of Proterozoic mafic dyke swarms: constraints from Th/Ta and La/Yb ratios. Precamb. Res. 81, 3–14.

de la Roche, H., 1965. Sur l'existence de plusieurs facies géochimiques dans les schistes paléozoïques des Pyrénées luchonnaises. Geol. Rundsch. 55, 274–301.

Dymek, R.F., Klein, C., 1988. Chemistry, Petrology and origin of banded iron-formation lithologies from 3800 Ma Isua supracrustal belt, West Greenland. Precamb. Res. 49, 247–302.

Fedele, L., Lustrino, M., Meluso, L., Morra, V., Zanetti, A., Vannucci, R., 2015. Trace-element partitioning between plagioclase, alkali feldspar, Ti-magnetite, biotite, apatite and evolved potassic liquids from Campi Flegrei (Southern Italy). Am. Min. 100, 233–249.

Ganno, S., Ngnotue, T., Kouankap, N.G.D., Nzenti, J.P., Notsa, F.M., 2015a. Petrology and geochemistry of the banded iron-formation from Ntem complex greenstones belt, Elom area, southern Cameroon: implications for the origin and depositional environment. Chemie der Erde 75, 375–387.

Ganno, S., Moudioh, C., Nzina Nchare, A., Kouankap Nono, G.D., Nzenti, J.P., 2015b. Geochemical fingerprint and iron ore potential of siliceous itabirite Paleoproterozoic Nyong series, Zambi area, southwestern Cameroon. Resour. Geol. 66, 71–80.

Ganno, S., Njiosseu Tanko, E.L., Kouankap Nono, G.D., Djoukouo, S.A., Moudioh, C., Ngnotué, T., Nzenti, J.P., 2017. A mixed sea water and hydrothermal origin of superior-type banded iron formation (BIF)-hosted Kouambo iron deposit, Paleoproterozoic Nypng series, southwestern Cameroon: constraints from petrography. Ore Geol. Rev. 80, 860–875.

Gonzalez, P.D., Sato, A.M., Llambias, E.J., Petronilho, L.A., 2009. Petrology and geochemistry of the banded iron formation in the eastern Sierras Pampeanas of San Luis (Argentina): implications for the evolution of the Nogoli metamorphic complex. J. South Am. Earth Sci. 28, 89–112.

Gross, G.A., McLeod, C.R., 1980. A preliminary assessment of the chemical composition of iron-formations in Canada. Can. Mineral. 18, 223–239.

Herron, M.M., 1988. Geochemical classification of terrigenous sands and shale from core or Log data. J. Sedim. Petrol. 58, 820–829.

Ilouga, D.C.I., Suh, C.E., Ghogomu, R.T., 2013. Textures and rare earth elements composition of banded iron formations (BIF) at Njweng, Mbalam iron ore district, southern Cameroon. Int. J. Geosci. 4, 146–165.

Kaufman, A.J., Johnston, D.T., Farquar, J., Masterson, A.L., Lyons, T.W., Bates, S., Anbar, A.D., Anold, G.L., Garvin, J., Buick, R., 2007. Late Archean biospheric oxygenation and atmospheric evolution. Science 317, 1900–1903.

Klein, C., 2005. Some Precambrian banded-iron formation (BIFs) from around the world: their age, geologic setting, mineralogy, metamorphism, geochemistry and origin. Am. Miner. 90, 1473–1499.

Konhauser, K.O., Amskold, L., Lalonde, S.V., Posth, N.R., Kappler, A., Anbar, A., 2007. Decoupling photochemical Fe(II) oxidation from shallow water BIF deposition. Earth Planet. Sci. Lett. 258, 87–100.

Leake, B.E., Woollet, A.R., Arps, C.E.S., Birch, W.D., Gilbert, M.C., Grice, J.D., Hawthorne, F.C., Kato, A., Kisch, H.J., Krivovichev, V.G., Linthout, K., Laird, J., Mandarino, J., Maresch, W.V., Nickel, E.H., Rock, N.M.S., Schumacher, J.C., Smith, D.C., Stephenson, N.C.N., Ungaretti, L., Whittaker, E.J.W., Youzhi, G., 1997. Nomenclature of amphiboles. Report of the subcommittee on Amphiboles of the International Mineralogical Association Commission on New Minerals and Mineral Names. Eur. J. Mineralogy 9, 623–651.

Lemarchand, F., Villemant, B., Calas, G., 1987. Trace element distribution coefficients in alkaline series. Geochim. Cosmochim. Acta 51, 1071–1081.

Martin, H., Smithies, R.H., Rapp, R., Moyen, J.F., Champion, D., 2005. An overview of adakite, tonalite-trondhjemite-granodiorite (TTG), and sanukitoid: relationships and some implications for crustal evolution. Lithos 79, 1–24.

McDonough, W.F., Sun, S.-S., 1995. The composition of earth. Chem. Geol. 120, 223–253.

Mclennan, S.M., 1989. Rare earth elements in sedimentary rocks: influence of provenance and sedimentary processes. In: Lipin, B.R., Mckay, G.R. (Eds.), Geochemistry and mineralogy of Rare Earth Elements, 21, Reviews in Mineralogy, Mineralogical Society of America, pp. 169–200.

Meschede, M., 1986. A method of discriminating between different types of mid-ocean ridge basalts and continental tholeiites with Nb-Zr-Y diagram. Chem. Geol. 56, 207–218.

Moyen, J.F., 2011. The composite Archaean grey gneisses: petrological significance and evidence for a non-unique tectonic setting for Archaean crustal growth. Lithos 123, 21–36.

Moyen, J.F., Martin, H., 2012. Forty years of TTG research. Lithos 148, 312–336.

Nesbitt, H.W., Young, G.M., 1982. Early Proterozoic climates and plate motions inferred from major element chemistry of lutites. Nature 299, 715–717.

Nforba, M.T., Kabeyene, K.V., Suh, C.E., 2011. Regolith geochemistry and mineralogy of the Mbalam itabirite-hosted iron ore district, southeastern Cameroon. Open J. Geol. 1, 17–36.

Ngako, V., Njonfang, E., 2011. Plates amalgamation and plate destruction, the western Gondwana history. In: Closson, D. (Ed.), Tectonics. (ISBN 978–953–307–545–7, InTech. Available from: http://www.intechopen.com/books/tectonics/plates-amalgamation-and-plate-destruction-the-westerngondwana-history).

Ngako, V., Affaton, P., Njongfang, E., 2008. Pan-African tectonics in northwestern Cameroon: implication for the history of western Gondwana. Gondwana Res. 14, 509–522.

Ngako, V., Jégouzo, P., Nzenti, J.P., 1991. Le Cisaillement Centre camerounais : rôle structural et géodynamique dans l'orogenèse panafricaine. C.R. Acad. Sci. Paris, Ser. II 313, 457–463.

Ngnotué, T., Nzenti, J.P., Barbey, P., Tchoua, F.M., 2000. The Ntui-Betamba high-grade gneisses: a northward extension of the Pan-African Yaoundé gneisses in Cameroon. J. Afric. Earth Sci. 31, 369–381.

Nkoumbou, C., Déruelle, B., Velde, D., 1995. Petrology of MT etinde nephelinite series. J. Petrol. 36, 373–395.

Nkoumbou, C., Barbey, P., Yonta-Ngouné, C., Paquette, J.L., Villiéras, F., 2014. Pre-collisional geodynamic context of the southern margin of the Pan-African fold belt in Cameroon. J. Afric; Earth Sci. 99, 245–260.

Nkoumbou, C., Villiéras, F., Barbey, P., Yonta-Ngouné, C., Joussemet, R., Diot, F., Njopwouo, D., Yvon, J., 2009. Ni-Co sulphide segregation in the Mamb pyroxenite intrusion, Cameroon. C. R. Geoscience 341, 517–525.

Nsoh, E.F., Agbor, A.T., Etame, J., Suh, C.E., 2014. Ore-textures and geochemistry of the Nkout iron deposit, South East Cameroon. Sci. Technol. Dev. 15, 43–52.

Pecoits, E., Gingras, M.K., Barley, M.E., Kappler, A., Posth, N.R., Konhauser, K.O., 2009. Petrography and geochemistry of the Dales Gorge banded iron formation: Paragenetic sequence, source and implications for paleo-ocean chemistry. Precamb. Res. 172, 163–187.

Pickard, A.L., Barley, M.E., Krapez, B., 2004. Deep-marine depositional setting of banded iron formation: sedimentological evidence from interbedded clastic sedimentary rocks in the Early Palaeoproterozoic Dales Gorge member of western Australia. Sediment. Geol. 170, 37–62.

Robb, L., 2005. Introduction to Ore-forming Processes. Blackwell publishing (373 pp.).

Simonson, B.M., 2003. Origin and evolution of large Precambrian iron formation. Geol. Soc. Am. 370, 231–244.

Suh, C.E., Cabral, A.R., Ndime, E., 2009. logy and ore fabric of the Nkout high-grade haematite deposit, southern Cameroon. In: Proceedings of the 10th Biennal of Smart Science for Exploration and Mining. pp. 558–560.

Suh, C.E., Cabral, A.R., Shemang, E.M., Mbinkar, L., Mboudou, G.G.M., 2008. Two contrasting iron deposits in the Precambrian mineral belt of Cameroon, West Africa. Explor. Min. Geol. 17, 197–207.

Tchakounté, J., 1999. Étude géologique de la région d'Etoundou-Bayomen dans la série métamorphique de Bafia : tectonique, géochimie, métamorphisme (Thèse 3ème cycle). Université de Yaoundé I, Cameroun (188 pp.).

Tchakounté, J.N., Toteu, S.F., Van Schmus, W.R., Penaye, J., Deloule, E., Mvondo-Ondoa, J., Bouyo Houketchang, M., Ganwa, A.A., White, W., 2007. Evidence of ca 1.6-Ga detrital zircon in the Bafia Group (Cameroon): Implication for the chronostratigraphy of the Pan-African Belt north on the Congo craton. C. R. Geoscience 339, 132–142.

Tchakounté, N.J., Eglinger, A., Toteu, F., Zeh, A., Nkoumbou, C., Mvondo-Ondoa, J., Barbey, P., 2017. The Early Neoproterozoic fragmentation of the Congo craton: The Adamawa-Yadé domain, a piece of Archaean crust in the Central African Orogenic Belt (Bafia area, Cameroon). Precamb. Res. (accepted).

Tchato, F.C., 2013. Pétrographie, chimico-minéralogie, géochimie et cadre géodynamique des amphibolites d'Itiitin-Ndikinimeki (Master's degree thesis). The University of Yaoundé I, Cameroon (78 pp.).

Tchato, D.T., Simeni Wambo, N.A., Keutchafo, N.A., Tchouankoué, J.P., Cuccinello, C., 2017. Gology, mineralogy and geochemistry of the Kekem dyke swarm (Western Cameroon): insights into Paleozoic-Mesozoic magmatism and geodynamic implications. C. R. Geoscience 349 (à paraître).

Tessontsap Teutsong, Tomaso, R.R., Bontognali, Ndjigui, P.D., Vrijmoed, Teagle, D., Cooper, M., Vance, D., 2017. Petrography and geochemistry of the Mesoarchean Bikoula banded iron formation in the Ntem complex (Congo craton), southern Cameroon: implications for its origin. Ore Geol. 80, 267–388.

Toteu, S.F., Van Schmus, W.R., Penaye, J., Michard, A., 2001. New U–Pb and Sm–Nd data from North-Central Cameroon and its bearing on the Pre-Pan African history of central Africa. Precamb. Res. 67, 321–347.

Toteu, S.F., Yongue Fouateu, R., Penaye, J., Tachakounté, J., Seme Mouangue, A.C., Van Schmus, W.R., Deloule, E., Stendal, H., 2006. U-Pb dating of plutonic rocks involved in the nappe tectonic in southern Cameroon: consequence for the Pan-African orogenic evolution of the central African fold belt. J. Afr. Earth Sci. 44, 479–493.

Trendall, A., 1983. The Hamersley basin. In: Trendall, A., Morris, R. (Eds.), Iron-formation: facts and problems. Elsevier, Amsterdam, pp. 69–129.

Wonder, J., Spry, P., Windom, K., 1988. Geochemistry and origin of manganese-rich rocks related to iron-formation and sulfide deposits, western Georgia. Econ. Geol. 83 (5), 1070–1081.